Progress of Theoretical Physics, Vol. 98, No. 1, July 1997

Infra-Red Fixed Points in an Asymptotically Non-Free Theory

Masako BANDO, Joe SATO* and Koichi YOSHIOKA**

Aichi University, Miyoshi-cho, Aichi 470-02
**Institute for Cosmic Ray Research, The University of Tokyo, Tanashi 188*
***Department of Physics, Kyoto University, Kyoto 606-01*

(Received March 14, 1997)

We investigate the infrared fixed point structure in asymptotically free and asymptotically non-free theory. We find that the ratios of couplings converge strongly to their infrared fixed points in the asymptotically non-free theory.

§1. Introduction

The manner in which the Yukawa couplings reproduce the masses of quarks and leptons is one of the unsolved problems in particle physics. These masses may be constrained by requiring some symmetry or by imposing grand unified theory and/or they may be related to gauge couplings. The latter is strongly indicated by the top quark mass. About 3 years ago, Lanzagorta and Ross [1] attempted to determine the relation between Yukawa couplings and gauge couplings through the infrared fixed point structure. This method in which the infrared fixed points may determine the heavy fermion masses was first proposed by Pendleton and Ross. [2] However, such an infrared fixed point has rarely been reached in usual asymptotically free (AF) standard models because of the infrared divergent character. [3] Furthermore, since the coupling constants become very large in the low energy region, the perturbative treatment is no more guaranteed in the infrared region.

More than 40 years ago, Landau proposed an attractive idea that low energy physics may be determined with an asymptotically non-free (ANF) theory. He illustrated this idea by showing the possibility to obtain a very small fine structure constant. This idea was applied to determine the ratio of gauge couplings. [4] In particular, it was pointed out by Moroi et al. [5] that the minimal supersymmetric standard model (MSSM) with 1 extra vector-like family (EVF) gives the observed ratio of the gauge couplings (Weinberg angle).

In a previous paper, [6] we investigated a possible scenario of the standard gauge symmetry with ANF character and showed that due to the ANF gauge couplings the top Yukawa coupling is quite insensitive to their initial values fixed at GUT scale M_G. We would like to stress that such strong convergence of Yukawa couplings to their infrared fixed points is a common feature appearing in ANF theories.

In this paper we investigate how strongly the couplings are focused into their infrared points in ANF theories and demonstrate the structure of the renormalization-group flow. As illustrations we take the supersymmetric standard models with AF and ANF gauge couplings and compare them by concentrating on their infrared

structure.

§2. Infrared structure of AF and ANF theories

Before studying realistic (AF and ANF) models we first consider a simple gauged Yukawa system which has one gauge coupling g and one Yukawa coupling y, whose 1-loop β-functions are

$$\frac{d\alpha}{dt} = -\frac{b}{2\pi}\alpha^2, \tag{2·1}$$

$$\frac{d\alpha_y}{dt} = \frac{\alpha_y}{2\pi}\Big(a\alpha_y - c\alpha\Big), \tag{2·2}$$

where

$$\alpha \equiv \frac{g^2}{4\pi}, \quad \alpha_y \equiv \frac{y^2}{4\pi}, \qquad t = \ln\left(\frac{\mu}{\mu_0}\right). \tag{2·3}$$

The system is asymptotically free (asymptotically non-free) for $b > 0$ ($b < 0$) and always $a > 0$, $c \geq 0$. From these, we obtain

$$\frac{dR}{dt} = \frac{a}{2\pi}\alpha R(R - R^*), \qquad \left(R \equiv \frac{\alpha_y}{\alpha}\right) \tag{2·4}$$

$$R^* = \frac{c-b}{a}. \tag{2·5}$$

Since we would like to see the manner in which couplings reach infrared fixed points from their values at the GUT scale M_G, we take $\mu_0 = M_G$ and $\alpha(0) = \alpha(M_G)$. Then we obtain from (2·4) [6]

$$\frac{R(t) - R^*}{R(t)} = \left(\frac{\alpha(t)}{\alpha(M_G)}\right)^B \left(\frac{R(M_G) - R^*}{R(M_G)}\right), \tag{2·6}$$

$$B \equiv 1 - \frac{c}{b}. \tag{2·7}$$

Here, R^* is an infrared fixed point if $R^* > 0$. This is equivalent to what Lanzagorta and Ross derived in Ref. 1). From this equation, we see that the suppression factor $\xi \equiv \left(\frac{\alpha(t)}{\alpha(M_G)}\right)^B$ provides the criterion on rate at which R approaches the infrared fixed point value R^*. Note that this factor is independent of the detailed information of the system and is determined from gauge coupling alone. The b-dependence of the suppression factor ξ is shown in Fig. 1, from which we find a large difference between AF ($b > 0$) and ANF ($b < 0$) cases. In the AF case the point $b = c$ at which B becomes 0 corresponds to $\xi = 1$. If we dare to extrapolate our formula above this critical point, ξ becomes larger than 1, but R^* becomes negative and is no more an

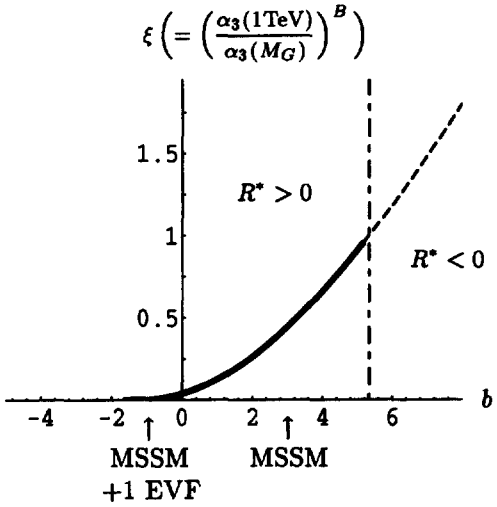

Fig. 1. Typical behavior of the suppression factor ξ by taking $\alpha = \alpha_3$. ($\alpha_3(M_Z) = 0.12$, $c = \frac{16}{3}$)

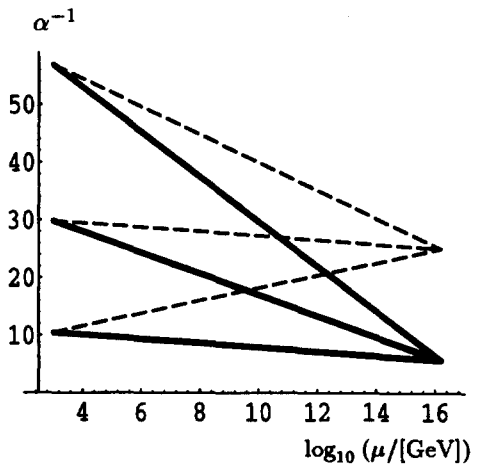

Fig. 2. Typical μ-dependence of $\alpha_1(\mu)$, $\alpha_2(\mu)$, $\alpha_3(\mu)$ in the MSSM (dashed lines) and the MSSM + 1 EVF (solid lines).

infrared fixed point. From (2·6) we see that ξ blows up and $R(t)$ tends to zero in the low energy limit.[7] On the other hand, in the ANF case there is always a non-trivial infrared fixed point $R^*(> 0)$, and convergence to R^* becomes much better.

Now we illustrate the difference in behavior of the AF and ANF theories by applying this formula to two models, the minimal supersymmetric standard model and the MSSM with one extra vector-like family (EVF).[4)-6)] Typical behavior of the running gauge couplings is shown in Fig. 2. They are unified at the same scale in the two cases, but with different unified couplings.

Let us first exhibit typical values for the AF and ANF cases, taking $\alpha = \alpha_3$, $\alpha_y = \alpha_t$ with a realistic value of α_3 (see §3 for details),

$$\text{MSSM} \quad : \quad b = 3, \quad c = \frac{16}{3} \quad \Rightarrow \quad B = -\frac{7}{9}$$

$$\left(\frac{\alpha_3(M_Z)}{\alpha_3(M_G)}\right)^B \sim \left(\frac{0.12}{0.04}\right)^{-7/9} \sim 0.43, \qquad (2\cdot8)$$

$$\text{MSSM} + 1 \text{ EVF} \quad : \quad b = -1, \quad c = \frac{16}{3} \quad \Rightarrow \quad B = \frac{19}{3}$$

$$\left(\frac{\alpha_3(M_Z)}{\alpha_3(M_G)}\right)^B \sim \left(\frac{0.12}{1.0}\right)^{19/3} \sim 10^{-6}. \qquad (2\cdot9)$$

The suppression factors can be read off Fig. 1 (indicated by arrows). We can see the situation more clearly by comparing the μ-dependence of α_t/α_3 in the AF and ANF cases. In the MSSM + 1 EVF, the convergence to the infrared fixed point is much better than that in the MSSM, and its fixed point value depends very weakly on the initial value at M_G (Fig. 4). This is because gauge couplings are asymptotically non-free and their unified coupling is very large at M_G (Fig. 2).

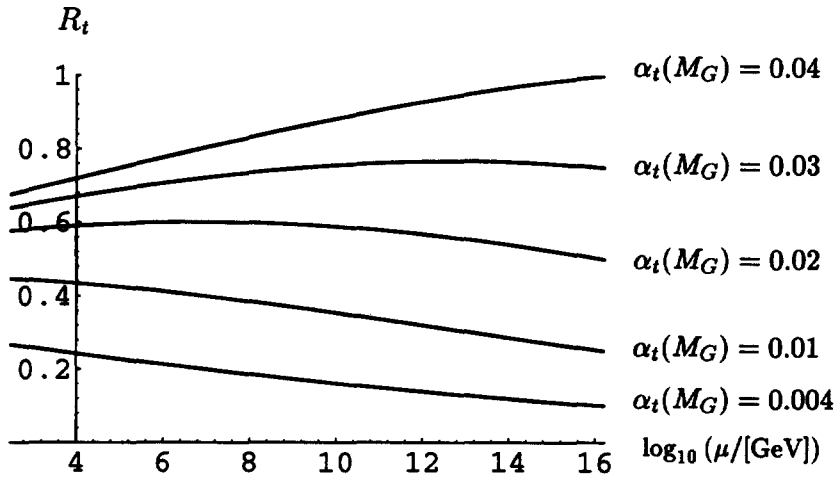

Fig. 3. R_t in the MSSM. ($M_G = 1.6 \times 10^{16}$ GeV, $\alpha_G = 0.04$)

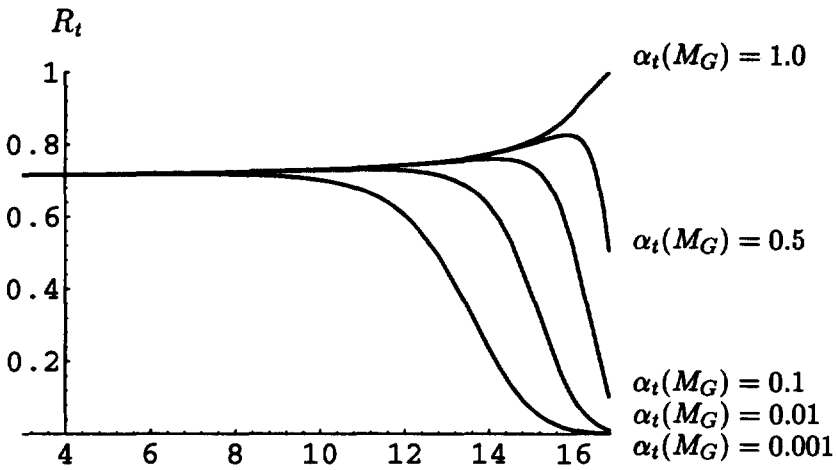

Fig. 4. R_t in the MSSM + 1 EVF. ($M_G = 7.0 \times 10^{16}$ GeV, $\alpha_G = 1.0$)

Next we investigate the RG flow in the (α_3, α_t) plane. The RG flow behaves quite differently according to the regions separated by the fixed line $\alpha_t/\alpha_3 = R_t^*$ (Figs. 5 and 6).

In the lower region of the AF case, the Yukawa coupling, as well as the gauge coupling, is found to be asymptotically free, and we have a non-trivial continuum limit.[7] Although the ratio finally approaches the infrared fixed point, in the infrared region both of the couplings become very large, and the one-loop approximation is no longer reliable.

For the other situations, either or both couplings are divergent at high energy. In the lower region of the ANF case the gauge coupling governs the Yukawa coupling very strongly. The gauge coupling diverges at some high energy scale. In the upper region for both cases, on the other hand α_t diverges at some high energy scale.

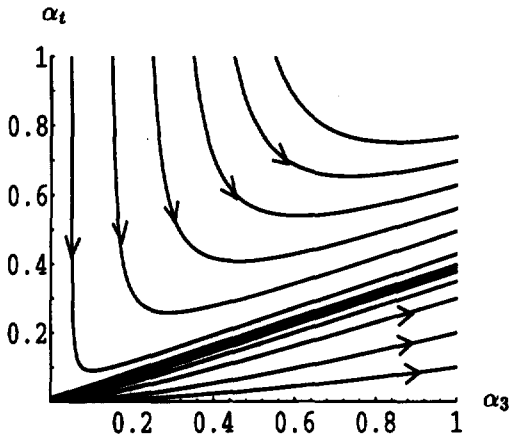

Fig. 5. RG flow diagram in the MSSM. The arrows denote the flow directiond toward the infrared region and the bold lines indicate the fixed lines.

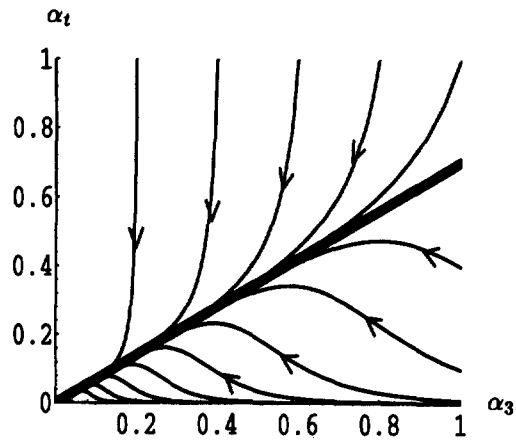

Fig. 6. RG flow diagram in the MSSM+1 EVF. The arrows and the bold lines represent the same as in Fig. 5.

Then the theory becomes trivial in the continuum limit and we should make use of cutoff theory. The former corresponds to dynamical gauge boson [8] and the latter, dynamical Higgs boson. [9]

It is noted that the ANF case is in strong contrast with the AF case. In both the upper and lower regions, the ratio evidently has an infrared fixed point where the one-loop approximation becomes more and more valid. This can be clearly seen in Fig. 6. This infrared stability is very attractive and may make the determination of Yukawa coupling constants feasible.

§3. Infrared solutions of MSSM + 1 EVF

Keeping the above attractive features in mind, we further undertake an analysis of the infrared fixed point solutions of MSSM + 1 EVF, which includes three gauge and Yukawa couplings. We suppose that the superpotential takes the form

$$W = W_3 + W_4 + W_{\bar{4}}\,, \tag{3·1}$$

$$W_3 = y_{t_3} Q_3 H \bar{t}_3 + y_{b_3} Q_3 \bar{H} \bar{b}_3 + y_{\tau_3} L_3 \bar{H} \bar{\tau}_3\,, \tag{3·2}$$

$$W_4 = y_{t_4} Q_4 H \bar{t}_4 + y_{b_4} Q_4 \bar{H} \bar{b}_4 + y_{\tau_4} L_4 \bar{H} \bar{\tau}_4\,, \tag{3·3}$$

$$W_{\bar{4}} = y_{\bar{t}} \bar{Q} \bar{H} t_{\bar{4}} + y_{\bar{b}} \bar{Q} H b_{\bar{4}} + y_{\bar{\tau}} \bar{L} H \tau_{\bar{4}}\,, \tag{3·4}$$

and the Yukawa couplings satisfy*)

$$y_{t_3} = y_{t_4} \equiv y_t\,, \quad y_{b_3} = y_{b_4} \equiv y_b\,, \quad y_{\tau_3} = y_{\tau_4} \equiv y_\tau\,, \tag{3·5}$$

$$y_{\bar{t}} = y_{\bar{b}} = y_{\bar{\tau}} = 0\,. \tag{3·6}$$

*) The relations are always satisfied once we put these relations at M_G.

With these assumptions, there exist parameter regions where both the low-energy experimental values and the high energy GUT-like boundary conditions are consistently described.[6] Then the 1-loop β-functions for the ratio of the couplings to α_3 ($R_i \equiv \alpha_i/\alpha_3$) are

$$\frac{dR_1}{dt} = \frac{1}{2\pi}\alpha_3 R_1\Big(10.6R_1 - 1\Big), \tag{3·7}$$

$$\frac{dR_2}{dt} = \frac{1}{2\pi}\alpha_3 R_2\Big(5R_2 - 1\Big), \tag{3·8}$$

$$\frac{dR_t}{dt} = \frac{1}{2\pi}\alpha_3 R_t\left(9R_t + R_b - \frac{13}{15}R_1 - 3R_2 - \frac{19}{3}\right), \tag{3·9}$$

$$\frac{dR_b}{dt} = \frac{1}{2\pi}\alpha_3 R_b\left(R_t + 9R_b + 2R_\tau - \frac{7}{15}R_1 - 3R_2 - \frac{19}{3}\right), \tag{3·10}$$

$$\frac{dR_\tau}{dt} = \frac{1}{2\pi}\alpha_3 R_\tau\left(6R_b + 5R_\tau - \frac{9}{5}R_1 - 3R_2\right). \tag{3·11}$$

First we comment with regard to the infrared structure of R_τ. The naive infrared fixed point solution from all these β-functions should not be interpreted as the true fixed point, since this solution of R_τ is negative ($R_\tau^* \sim -0.66$). In this case, as was mentioned above, R_τ does not reach the non-trivial infrared fixed point, but rather zero, in the low energy limit (Fig. 7).

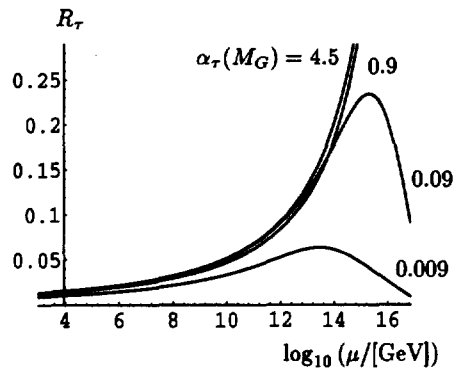

Fig. 7. R_τ in the MSSM + 1 EVF. ($M_G = 7.0 \times 10^{16}$ GeV, $\alpha_G = 1.0$)

In order to obtain the correct infrared fixed point solutions, we first set $R_\tau \sim 0$ and use the four remaining β-functions [(3·7) $\sim$ (3·10)]. The results are as follows:*)

$$R_1^* = 0.0943, \quad R_2^* = 0.2,$$
$$R_t^* = 0.702, \quad R_b^* = 0.697. \tag{3·12}$$
$$(R_\tau \sim 0.0)$$

From Figs. 4 and 8, we find that these quantities indeed reach their fixed points. As we mentioned before, these values are affected little by the initial values at M_G because of the asymptotically non-free gauge couplings. We are confident that the infrared fixed points obtained from these solutions are physically significant and provide us with reliable low-energy parameters.

*) Strictly speaking, R_1 and R_2 do not converge to their fixed point values. However, the differences $R_i(1\text{ TeV}) - R_i^*$ ($i = 1, 2$) are small enough for us to use the result (3·12).

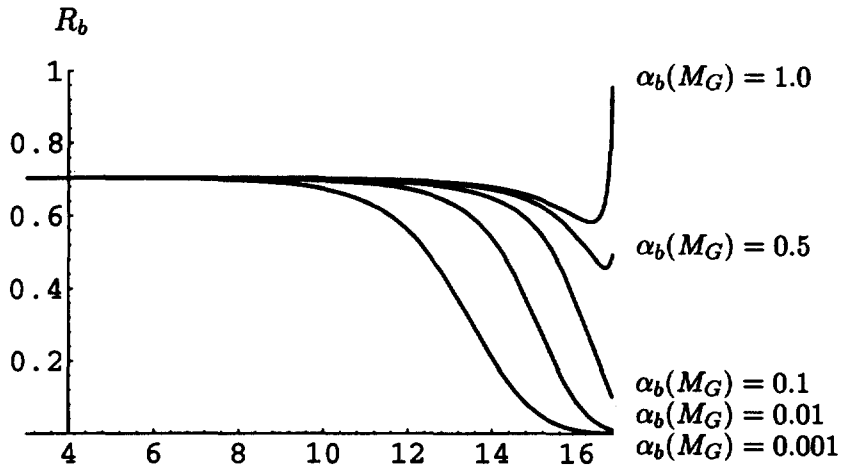

Fig. 8. R_b in the MSSM + 1 EVF. ($M_G = 7.0 \times 10^{16}$ GeV, $\alpha_G = 1.0$)

In the case at hand, by using these fixed point solutions and the experimental value of $\alpha_3(1\text{ TeV}) \sim 0.093$, we obtain, for example,*)

$$m_t(M_Z) \sim 178\text{ GeV}, \quad m_b(M_Z) \sim 3.2\text{ GeV}. \qquad (3\cdot13)$$
$$(\tan\beta \sim 58)$$

These values are certainly consistent with the experimental values[10]

$$m_t(M_Z) \sim 180 \pm 10\text{ GeV}, \quad m_b(M_Z) \sim 3.1 \pm 0.4\text{ GeV}. \qquad (3\cdot14)$$

§4. Conclusion

We found interesting infrared structure which is commonly seen in ANF theories. This is an important difference between AF and ANF theories. This possibility has long been observed but has never been taken serious.

The existence of extra fermions has been discussed from various points of view: in deriving CP violation, dynamical SUSY breaking, hierarchical mass matrix, and so on. In particular, GUT models beyond standard models, including string models and supergravity models, predict additional fermions quite naturally. We can expect that at low energy, the theory is asymptotically non-free.

We would like to stress that since ANF theories have strong predictive powers because of the strong convergence of couplings (ratio of couplings) to infrared fixed points, their study is considered important.

Acknowledgements

The authors would like to express their sincere thanks to T. Kugo and T. Yanagida for their valuable comments and encouragement. The previous work with

*) The value $\tan\beta \sim 58$ is determined from the experimental value $m_\tau(M_Z)$.[6]

T. Takeuchi and T. Onogi (as well as J. S. and M. B.) has provided a strong motivation for this work, and discussions with them were instructive. A part of this work was performed during the Kashikojima Workshop held in August 1996 at Kashikojima Center, which was supported by a Grand-in-Aid for Scientific Research (No. 07304029) from the Ministry of Education, Science and Culture. M. B. is supported in part by the Grand-in-Aid for Scientific Research (No. 33901-06640416) from the Ministry of Education, Science and Culture.

References

1) M. Lanzagorta and G. G. Ross, Phys. Lett. **349B** (1995), 319.
2) B. Pendleton and G. G. Ross, Phys. Lett. **98B** (1981), 291.
3) C. T. Hill, Phys. Rev. **D24** (1981), 691.
4) L. Maiani, G. Parisi and R. Petronzio, Nucl. Phys. **B136** (1978), 115.
5) T. Moroi, H. Murayama and T. Yanagida, Phys. Rev. **D48** (1993), 2995.
6) M. Bando, J. Sato, T. Onogi and T. Takeuchi, hep-ph/9612493.
7) M. Harada, Y. Kikukawa, T. Kugo and H. Nakano, Prog. Theor. Phys. **92** (1994), 1161.
8) T. Saito and K. Shigemoto, Prog. Theor. Phys. **57** (1977), 242.
H. Terazawa, K. Akama and Y. Chikashige, Phys. Rev. **D15** (1977), 480.
M. Bando, Y. Taniguchi and S. Tanimura, hep-th/9610244.
9) V. A. Miranskii, M. Tanabashi and K. Yamawaki, Phys. Lett. **221B** (1989), 177.
W. A. Bardeen, C. T. Hill and M. Lindner, Phys. Rev. **D41** (1989), 1647.
M. Bando, T. Kugo, N. Maekawa, N. Sasakura, Y. Watabiki and K. Suehiro, Phys. Lett. **246B** (1990), 466.
M. Bando, T. Kugo, N. Maekawa and H. Nakano, Phys. Rev. **D44** (1991), 2957.
10) Particle Data Group, Phys. Rev. **D54** (1996), 1.